



Measurements of high- n transitions in intermediate mass kaonic atoms by SIDDHARTA-2 at DAΦNE

F. Sgaramella^{1,a}, M. Tüchler^{2,3,b}, C. Amsler², M. Bazzi¹, D. Bosnar⁴, M. Bragadireanu⁵, M. Cargnelli², M. Carminati^{6,7}, A. Clozza¹, G. Deda^{6,7}, R. Del Grande^{1,8}, L. De Paolis¹, L. Fabbietti⁸, C. Fiorini^{6,7}, I. Friščić⁴, C. Guaraldo¹, M. Iliescu¹, M. Iwasaki⁹, A. Khreptak^{1,10}, S. Manti¹, J. Marton², M. Miliucci¹, P. Moskal^{10,11}, F. Napolitano¹, S. Niedźwiecki^{10,11}, H. Ohnishi¹², K. Piscicchia^{1,13}, Y. Sada¹², A. Scordo^{1,c}, H. Shi², M. Silarski¹⁰, D. Sirghi^{1,5,13}, F. Sirghi^{1,5}, M. Skurzok^{10,11}, A. Spallone¹, K. Toho¹², O. Vazquez Doce¹, E. Widmann², C. Yoshida¹², J. Zmeskal², C. Curceanu¹

¹ INFN-LNF, Istituto Nazionale di Fisica Nucleare-Laboratori Nazionali di Frascati, Frascati 00044, Roma, Italy

² Stefan-Meyer-Institut für Subatomare Physik, Vienna 1030, Austria

³ University of Vienna, Vienna Doctoral School in Physics, Vienna 1090, Austria

⁴ Department of Physics, Faculty of Science, University of Zagreb, 10000 Zagreb, Croatia

⁵ Horia Hulubei National Institute of Physics and Nuclear Engineering IFIN-HH Măgurele, Măgurele, Romania

⁶ Politecnico di Milano, Dipartimento di Elettronica, Informazione e Bioingegneria, Milano 20133, Italy

⁷ INFN Sezione di Milano, 20133 Milan, Italy

⁸ Physik Department E62, Technische Universität München, Garching 85748, Germany

⁹ RIKEN, Tokyo 351-0198, Japan

¹⁰ Faculty of Physics, Astronomy, and Applied Computer Science, Jagiellonian University, Krakow 30-348, Poland

¹¹ Center for Theranostics, Jagiellonian University, Krakow, Poland

¹² Research Center for Electron Photon Science (ELPH), Tohoku University, Sendai 982-0826, Japan

¹³ Centro Ricerche Enrico Fermi-Museo Storico della Fisica e Centro Studi e Ricerche “Enrico Fermi”, Roma 00184, Italy

Received: 16 December 2022 / Accepted: 10 March 2023

© The Author(s), under exclusive licence to Società Italiana di Fisica and Springer-Verlag GmbH Germany, part of Springer Nature 2023

Communicated by Klaus Peters

Abstract The SIDDHARTA-2 experiment installed at the DAΦNE collider of INFN-LNF performed, for the first time, measurements of high- n transitions in intermediate mass kaonic atoms during the data taking campaigns of 2021 and 2022. Kaonic carbon, oxygen, nitrogen and aluminium transitions, which occur in the setup materials, were measured by using the kaons stopped in the gaseous helium target cell with aluminium frames and Kapton walls, and are reported in this paper. These new kaonic atoms measurements add valuable input to the kaonic atoms transitions data base, which is used as a reference for theories and models of the low-energy strong interaction between antikaon and nuclei. Moreover, these results pave the way for future dedicated kaonic atoms measurements through the whole periodic table and to a new era for the antikaon-nuclei studies at low energy.

1 Introduction

Kaonic atoms represent an ideal tool to study the low-energy regime of Quantum Chromodynamics (QCD) in the strangeness sector, which cannot be described with a perturbative approach. They enable to directly access the K^-N interaction at threshold, without the need of an extrapolation as in the case of scattering experiments, since the relative energy between the kaon and the nucleus is already at the level of few keV. This access is crucial to constrain and unify the theoretical descriptions of this interaction.

Kaonic atoms have been studied intensely in the 1970s and 1980s, with measurements spanning over a wide range of elements in the periodic table, from lithium to uranium [1–12]. These measurements serve as database for low-energy antikaon-nuclei studies, constraining the theoretical descriptions of the K^-N interaction potential [13, 14]. However, the available data are affected by large experimental uncertainties and several measurements were proven to be at variance with more recent measurements employing modern detector technology, while many more kaonic atoms transitions are not yet measured [14]. For these reasons, starting in the

^a e-mail: francesco.sgaramella@lnf.infn.it (corresponding author)

^b e-mail: marlene.tuechler@oeaw.ac.at

^c e-mail: alessandro.scordo@lnf.infn.it

late 1990s, a new era of kaonic atoms studies was initiated by the KpX experiment at KEK in Japan, followed by the DEAR and SIDDHARTA experiments at DAΦNE, initially motivated by the so-called “kaonic hydrogen puzzle” [15–17], which was eventually solved by these experiments. The puzzle consisted of the fact that measurements performed on kaonic hydrogen in the 1970s and 1980s had found an attractive-type interaction [18–20], in contradiction with the analyses of low-energy scattering data [21–23]. Similarly, the early data for the kaonic helium-4 $2p$ level shift (see [1, 24]) showed a $> 5\sigma$ discrepancy with theoretical expectations [13, 25], the so-called “kaonic helium puzzle”. The puzzle was resolved in 2007 by the measurement of the E570 experiment at KEK [15], later confirmed by the SIDDHARTA collaboration [26]. These examples suggest that the current collection of data from the old experiments is not reliable, and new measurements with higher accuracy and state-of-the-art detectors are required to provide well grounded experimental input to theory.

The SIDDHARTA-2 experiment at the DAΦNE collider of Laboratori Nazionali di Frascati (INFN-LNF) in Italy is performing high precision kaonic atoms measurements. In 2019, the apparatus was installed on the collider with the main aim to measure the $2p \rightarrow 1s$ transition in kaonic deuterium. During the optimization phase of the collider and of the setup performances in 2021 and 2022, data were collected both with a reduced setup called SIDDHARTINO, which differs in the number of used Silicon Drift Detector (SDD) arrays, and with the full SIDDHARTA-2 setup. To optimize the setup parameters, various measurements were performed with different ^4He target gas densities [27].

The target cell consists of an aluminium frame with Kapton foil walls and contains gaseous helium, where the kaons produced by ϕ -decays are stopped. As a result, multiple kaonic atoms lines are present in the measured X-ray spectra, besides those of kaonic helium.

In this work, measurements of several intermediate mass kaonic atoms, such as kaonic carbon, oxygen, nitrogen, and aluminium high- n transition energies are reported, which also represent the first measurements ever for the reported transitions.

2 The experimental apparatus

DAΦNE [28], a double ring e^+e^- collider at INFN-LNF, provides an ideal environment for precision measurements of kaonic atoms, since it operates at the centre-of-mass energy of $1.02 \text{ GeV}/c^2$ and hence produces ϕ -mesons almost at rest. The charged kaon pairs from ϕ -decays, produced with a branching ratio of 49.1%, are therefore emitted in an almost back-to-back topology with momenta of $\sim 127 \text{ MeV}/c$ and low momentum spread ($\delta p/p \sim 0.1\%$). The SID-

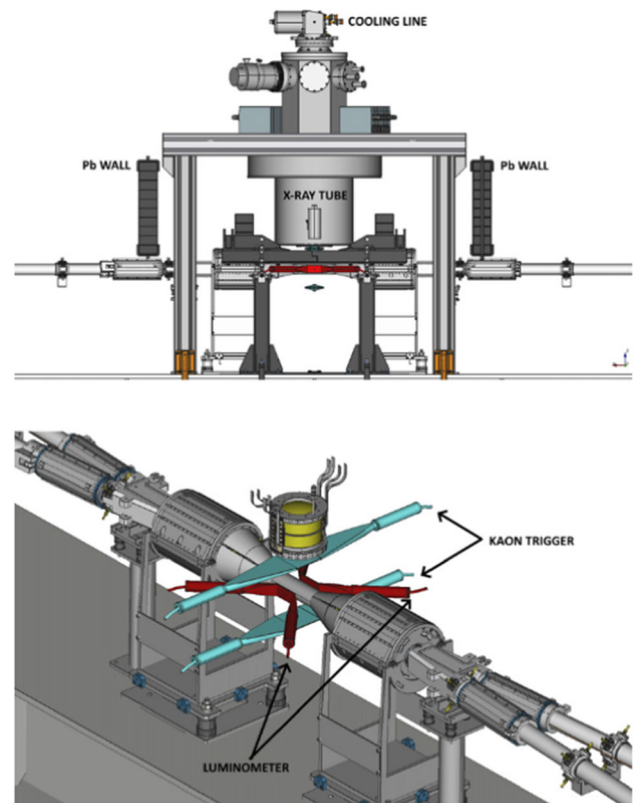


Fig. 1 Top: Schematic of the SIDDHARTINO experimental apparatus installed at the DAΦNE interaction point Bottom: Detailed view of the kaon trigger system (cyan), the luminosity monitor (red) and the target cell (yellow) surrounded by SDDs [27]

DHARTINO experimental apparatus, installed at the interaction point (IP) of the DAΦNE collider, was used for the commissioning of the setup from January 2021 to July 2021, which was followed by the installation of the full SIDDHARTA-2 apparatus and subsequent data taking in April - July 2022.

A schematic view of the SIDDHARTINO experimental apparatus is shown in the top panel of Fig. 1. To suppress the asynchronous background by taking advantage of the back-to-back K^+K^- emission, a kaon trigger (KT) system, consisting of two scintillators with photomultiplier (PMT) readout, is employed, one scintillator being placed below the beam pipe and the other one above, directly in front of the entrance window of the vacuum chamber, as shown in the bottom panel of Fig. 1. Only triggered events, where two signals are detected in coincidence by the two scintillators are detected, while the others are discarded. To monitor the beam quality and background in real-time, a luminosity monitor built with plastic scintillators and based on J-PET technology is implemented [29–33]. The luminometer takes advantage of the difference in the time of flight from the interaction point to the detector, between the Minimum Ionizing Particles (MIPs), originating from e^+ and e^- lost by the beams,

and kaons. Lead shielding, placed around the vacuum chamber, further suppresses background originating from beam losses and consequent bremsstrahlung. Inside the vacuum chamber, the kaonic atoms are produced inside a cylindrical, lightweight target cell cooled down to ~ 25 K. The target cell has a height of 125 mm and a diameter of 144 mm, and consists of high-purity aluminium bars together with ~ 150 μm thick Kapton sidewalls and a 125 μm thick Kapton entrance window.

The X-ray detection system surrounds the target cell. It contains large-area Silicon Drift Detector arrays, developed by Fondazione Bruno Kessler (FKB) in Trento, Politecnico di Milano, INFN-LNF and the Stefan Meyer Institute (SMI) in Vienna. Each array features 2×4 SDD cells with an active area of 0.64 cm^2 each. Figure 2 shows one SDD array. For the SIDDHARTINO setup, 8 SDD arrays and hence 64 read-out channels with a total active area of 41 cm^2 are employed; for SIDDHARTA-2, 48 arrays are used, with 384 read-out channels and a total active area of 246 cm^2 . Each SDD signal is amplified by CUBE [34], installed on ceramic carrier structures behind the detectors. The signals are read out and processed by a dedicated ASIC chip called SFERA [35,36]. For in-situ calibration of the SDDs, two X-ray tubes are implemented and periodic calibration runs are performed by the activation of high-purity Ti–Cu foils, mounted on the target cell. The fluorescence lines from these foils are then used for the online calibration of the detectors [37]. The SDD system was optimized and characterized in terms of its spectroscopic and timing response, showing a linearity better than 3 eV in the energy range 4–14 keV, an energy resolution of $(157.8 \pm 0.3 \pm 0.2)$ eV at 6.4 keV [38] and a long-term stability at the level of 2–3 eV [37], which fulfilled the requirements for the challenging measurements of light kaonic atoms. The final SIDDHARTA-2 setup for the planned kaonic deuterium measurement will employ additional measures for the suppression of background in the form of active, multiple-stage veto systems [39], which were not yet implemented during the measurements reported in this work, to enable a direct



Fig. 2 Silicon drift detector array for the SIDDHARTA-2 experiment with eight read-out cells indicated by the grey lines. The array is mounted on a ceramic carrier

comparison with the conditions of past kaonic helium experiments [40].

3 Data analysis

Data were accumulated with the helium gas target for a total integrated luminosity of 76 pb^{-1} . The first run took place with SIDDHARTINO during the beam optimization phase of DAΦNE in Spring 2021 and was dedicated to optimize the collider and setup performances. Following this run, a new kaonic helium measurement was performed with the complete SIDDHARTA-2 setup, to assess and adjust the experimental apparatus in view of the kaonic deuterium measurement planned to be performed in 2023.

Figure 3 shows the inclusive energy spectrum obtained by summing all the calibrated data collected with the SDDs. In the spectrum, the fluorescence X-ray transition lines from the activation of the setup materials by the particles lost from the beams are clearly seen. The Cu $K\alpha$ line was produced in the calibration foils on the target cell, while the Bi lines originate in the ceramic carriers behind the SDDs.

Since most of the background produced by DAΦNE is due to particles lost from the beams due to the Touschek effect, and thus is asynchronous with the K^+K^- production, it can be drastically reduced by using the kaon trigger. Only the X-ray SDD signals within a $5\text{ }\mu\text{s}$ time window with respect to the trigger signal can pass the selection (Trigger cut), resulting in a background reduction of a factor $1.3 \cdot 10^4$. The $5\text{ }\mu\text{s}$ time window was optimized for the front-end electronics which acquires and processes the signals coming from the SDDs.

The MIPs, originating from the beam-beam and beam-gas interactions can produce accidental trigger signals when passing through the two scintillators of the kaon trigger in coincidence. The K^+K^- pairs detected by the kaon trigger are identified by time of flight (ToF), allowing to distinguish whether a trigger signal is produced by kaons or MIPs. The

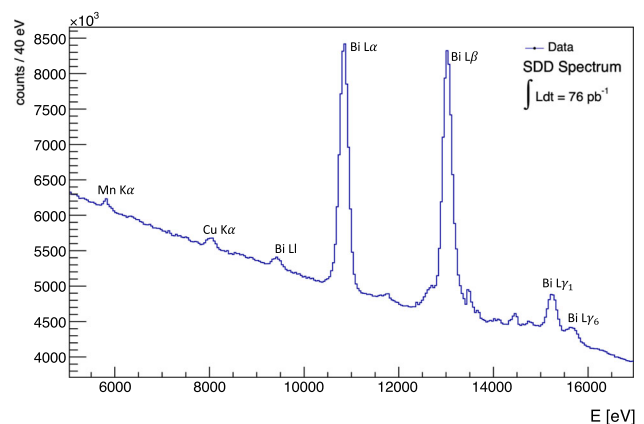


Fig. 3 Inclusive SDD energy spectrum

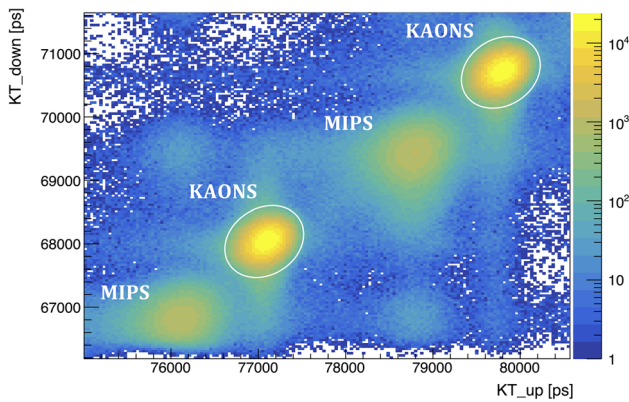


Fig. 4 Scatter plot of the time differences between the top (KT up) and bottom (KT down) scintillators of the kaon trigger and half the DAΦNE radio frequency (RF/2). The coincidence events related to kaons (high intensity) are clearly distinguishable from MIPS (low intensity). The double kaon and MIPS structures are due to the use of DAΦNE RF/2 as time reference (see text)

time difference between the trigger signal and the DAΦNE radiofrequency (RF), which provides a reference for each collision, was measured. Figure 4 shows the correlation of the mean time for the two scintillators of the kaon trigger. The K^+K^- pair events are clearly distinguishable from the MIPS (ToF cut). Since the ~ 370 MHz DAΦNE RF cannot be handled by the Constant Fraction Discriminators (CDF) used to process the kaon trigger signals, half the radio frequency (RF/2) was used as reference. Thus, every kaon trigger signal can be associated in time with one of the collisions that occurred over a CDF time period, and consequently the kaons and MIPS appear in two clusters, as shown in Fig. 4.

Finally, the time information provided by the SDDs was used to further reduce the electromagnetic background. Figure 5 shows the time difference between the kaon trigger signal and the X-ray hits on the SDDs for the SIDDHARTINO runs and the SIDDHARTA-2 runs. The peaks represent the X-ray events in coincidence with the kaon trigger, while the flat distribution results from uncorrelated events. The SDDs' timing resolution, which depends on the temperature [41], determines the acceptance window (Drift Time cut). For the SIDDHARTINO run, the SDDs' temperature was 170 K and the time window was 950 ns (FWHM) (Fig. 5 top). In the SIDDHARTA-2 run, the SDDs' temperature was reduced to 130 K, improving the time window to 450 ns (Fig. 5 bottom). Summing the data of all runs, this resulted in a further reduction of background by a factor two.

In Fig. 6, the X-ray spectrum of the summed data for the SIDDHARTINO and SIDDHARTA-2 runs after application of the event selections in Table 1 is shown. The kaonic atoms signals are now clearly visible. The peaks highlighted in the figure correspond to the X-ray emissions from kaonic atoms formed in the helium gas and in the components of the target cell.

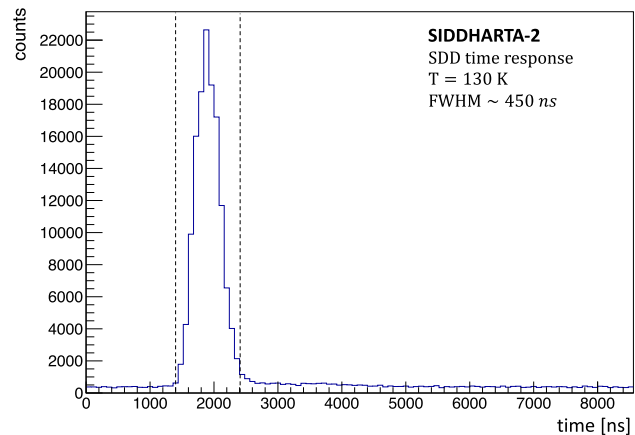
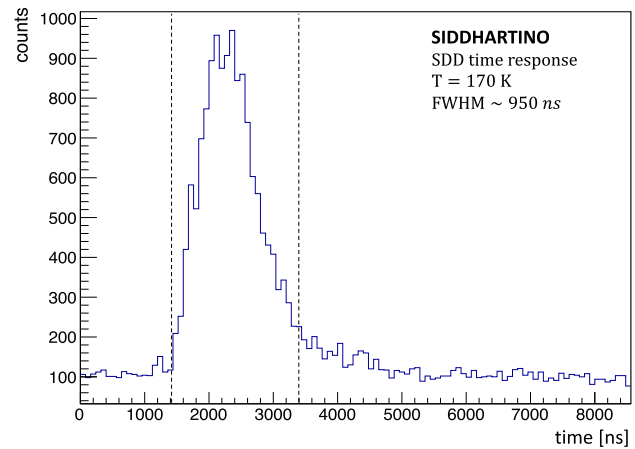


Fig. 5 Distribution of the time difference between the SDD X-rays hit and the trigger signals during the SIDDHARTINO (top), and the SIDDHARTA-2 (bottom) runs. The dashed lines represent the drift time window cut used to reduce the background

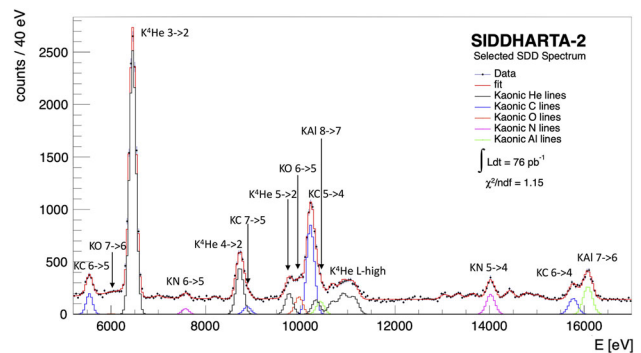


Fig. 6 SDD energy spectrum and fit of SIDDHARTA-2 and SIDDHARTINO summed data after background suppression (see text). The kaonic helium signals are seen as well as the kaonic carbon (KC), oxygen (KO), nitrogen (KN) and aluminium (KAl) peaks

The energy of each kaonic atoms transition was obtained from a fit of the spectrum. The SDDs' energy response for every transition line reported is described by the convolution of a Gaussian with an exponential function to reproduce the incomplete charge collection and electron-hole recombina-

Table 1 Data selection steps to reduce the background together with the number of events passing each requirement and the associated background rejection factor

Selection	Events	Rejection factor
No cut	$1.6 \cdot 10^9$	//
Trigger cut	118,598	$1.3 \cdot 10^4$
ToF cut	78,423	1.5
Drift time cut	39,163	2.0

Table 2 Kaonic carbon, oxygen, nitrogen and aluminium transition energies from the fit of the data in Fig. 6

Transition	Energy (eV)
$K^-C(6 \rightarrow 5)$	5541.7 ± 3.1 (stat) ± 2.0 (syst)
$K^-C(7 \rightarrow 5)$	8890.0 ± 13.0 (stat) ± 2.0 (syst)
$K^-C(5 \rightarrow 4)$	$10,216.6 \pm 1.8$ (stat) ± 3.0 (syst)
$K^-C(6 \rightarrow 4)$	$15,760.3 \pm 4.7$ (stat) ± 12.0 (syst)
$K^-O(7 \rightarrow 6)$	6016.0 ± 60.0 (stat) ± 2.0 (syst)
$K^-O(6 \rightarrow 5)$	9968.1 ± 6.9 (stat) ± 2.0 (syst)
$K^-N(6 \rightarrow 5)$	7577.0 ± 17.0 (stat) ± 2.0 (syst)
$K^-N(5 \rightarrow 4)$	$14,010.6 \pm 8.2$ (stat) ± 9.0 (syst)
$K^-Al(8 \rightarrow 7)$	$10,441.0 \pm 8.5$ (stat) ± 3.0 (syst)
$K^-Al(7 \rightarrow 6)$	$16,083.4 \pm 3.8$ (stat) ± 12.0 (syst)

tion effect [41], except for the kaonic helium lines, which were fitted with Voigt functions to account for the intrinsic linewidth of the transition due to the possible effect of the strong interaction. For the other high- n transition lines, the widening induced by strong interaction is known to be much below the resolution of our detectors [14].

In addition, two exponential plus a constant function are used to describe the background shape. The final fit function properly reproduces the data distribution, with a $\chi^2/\text{ndf} = 1.15$ in the energy range from 5 to 17 keV.

Several high- n transition energies in intermediate mass kaonic atoms, such as kaonic carbon, oxygen, nitrogen and aluminium are measured here for the first time. The discussion about kaonic helium transition energies goes beyond the scope of this article and for the SIDDHARTINO data is reported in [27]. The kaonic carbon, oxygen and nitrogen transitions are the result of kaons stopped in the Kapton walls, whereas the kaonic aluminium transitions were produced by kaons stopped in the top and bottom frames of the target cell. The final results for the kaonic C, O, N and Al transitions are shown in Table 2. The associated systematic uncertainties take into account the linearity and stability of the SDDs, as well as the effects produced by the energy calibration procedure, following the method described in [37,38]. Thus, various transitions are measured with a statistical precision

better than 10 eV, and for the majority of the measurements the systematic uncertainty is below 3 eV.

4 Conclusions

The SIDDHARTA-2 experiment performed high precision measurements of a series of intermediate mass kaonic atoms transitions, which also represent the first measurements ever for the reported transitions. Kaonic carbon, oxygen, nitrogen and aluminium X-ray transitions in the 5–16 keV energy range were measured during the 2021 and 2022 data taking campaigns, by using kaons stopped in the setup materials.

These new data enrich the kaonic atoms transitions database, which is used as input and as test-bed for theories and models of kaon-nuclei interactions at low energies, a field which is still far from being fully understood. The new data added by SIDDHARTA-2 can stimulate a revival of the theoretical activity in the field, towards a better understanding of the strong interaction with strangeness and of the role played by multi-nucleon absorption processes [14,42], with implications extending from particle and nuclear physics to astrophysics [39,43–45].

The series of measurements reported in this paper also show the potential of DAΦNE and SIDDHARTA-2 technologies to address high precision kaonic atoms measurements along the whole periodic table, within a future program which was already put forward by the scientific community [46,47].

Acknowledgements We thank C. Capocchia from LNF-INFN and H. Schneider, L. Stohwasser, and D. Pristauz-Telsnigg from Stefan Meyer-Institut for their fundamental contribution in designing and building the SIDDHARTA-2 setup. We thank as well the DAΦNE staff for the excellent working conditions and permanent support. We acknowledge support from the SciMat and qLife Priority Research Areas budget under the program Excellence Initiative-Research University at the Jagiellonian University. Part of this work was supported by the Austrian Science Fund (FWF): [P24756-N20 and P33037-N]; the EXOTICA project of the Ministero degli Affari Esteri e della Cooperazione Internazionale, PO21MO03; the Croatian Science Foundation under the project IP-2018-01-8570; the EU STRONG-2020 project (Grant Agreement No. 824093); the EU Horizon 2020 project under the MSCA (Grant Agreement 754496); the Japan Society for the Promotion of Science JSPS KAKENHI Grant No. JP18H05402; the Polish Ministry of Science and Higher Education grant No. 7150/E-338/M/2018 and the Polish National Agency for Academic Exchange (grant no PPN/BIT/2021/1/00037).

Data Availability Statement This manuscript has associated data in a data repository. [Authors' comment: The data that support the findings of this study are available upon reasonable request from the corresponding authors].

References

1. C.E. Wiegand, R.H. Pehl, Measurement of Kaonic X Rays from He-4. Phys. Rev. Lett. **27**, 1410–1412 (1971). <https://doi.org/10.1103/PhysRevLett.27.1410>

2. C. Batty et al., Measurement of kaonic and pionic X-rays from liquid helium. Nucl. Phys. A **326**, 455–462 (1979). [https://doi.org/10.1016/0375-9474\(79\)90403-2](https://doi.org/10.1016/0375-9474(79)90403-2)
3. C. Batty et al., Measurement of kaonic X-rays from Li, LiH AND Be. Nucl. Phys. A **282**, 487–492 (1977). [https://doi.org/10.1016/0375-9474\(77\)90072-0](https://doi.org/10.1016/0375-9474(77)90072-0)
4. G. Backenstoss et al., K- mass and K-polarizability from kaonic atoms. Phys. Lett. B **43**, 431–436 (1973). [https://doi.org/10.1016/0370-2693\(73\)90391-2](https://doi.org/10.1016/0370-2693(73)90391-2)
5. G. Backenstoss et al., Intensities and strong interaction attenuation of kaonic X-rays. Nucl. Phys. B **73**, 189–201 (1974). [https://doi.org/10.1016/0550-3213\(74\)90014-5](https://doi.org/10.1016/0550-3213(74)90014-5)
6. C. Batty et al., Measurement of strong interaction effects in kaonic atoms. Nucl. Phys. A **329**, 407–428 (1979). [https://doi.org/10.1016/0375-9474\(79\)90384-1](https://doi.org/10.1016/0375-9474(79)90384-1)
7. P. Barnes et al., Measurement of kaonic X-rays from Al, Si, Ni and Cu. Nucl. Phys. A **231**, 477–492 (1974). [https://doi.org/10.1016/0375-9474\(74\)90511-9](https://doi.org/10.1016/0375-9474(74)90511-9)
8. C. Wiegand, G. Godfrey, Measurements of x rays and γ rays from stopped kaons. Phys. Rev. A **9**, 2282 (1974). <https://doi.org/10.1103/PhysRevA.9.2282>
9. R. Kunselman, Kaon mass measurement from kaonic atom x-ray energies; the 4f–3d kaonic transition in chlorine. Phys. Lett. B **34**, 485–487 (1971). [https://doi.org/10.1016/0370-2693\(71\)90660-5](https://doi.org/10.1016/0370-2693(71)90660-5)
10. R. Kunselman, Negative—kaon mass. Phys. Rev. C **9**, 2469 (1974). <https://doi.org/10.1103/PhysRevC.9.2469>
11. C. Batty et al., Nuclear quadrupole deformation effects on pionic and kaonic X-rays. Nucl. Phys. A **355**, 383–402 (1981). [https://doi.org/10.1016/0375-9474\(81\)90534-0](https://doi.org/10.1016/0375-9474(81)90534-0)
12. S. Cheng et al., K-mass from kaonic atoms. Nucl. Phys. A **254**, 381–395 (1975). [https://doi.org/10.1016/0375-9474\(75\)90224-9](https://doi.org/10.1016/0375-9474(75)90224-9)
13. C. Batty, E. Friedman, A. Gal, Strong interaction physics from hadronic atoms. Phys. Rep. **287**, 385–445 (1997). [https://doi.org/10.1016/S0370-1573\(97\)00011-2](https://doi.org/10.1016/S0370-1573(97)00011-2)
14. E. Friedman, A. Gal, C.J. Batty, Density dependent K-nuclear optical potentials from kaonic atoms. Nucl. Phys. A **579**, 518–538 (1994). [https://doi.org/10.1016/0375-9474\(94\)90921-0](https://doi.org/10.1016/0375-9474(94)90921-0)
15. S. Okada et al., Precision measurement of the 3d \rightarrow 2p x-ray energy in kaonic He-4. Phys. Lett. B **653**, 387–391 (2007). <https://doi.org/10.1016/j.physletb.2007.08.032>
16. M. Iwasaki et al., Observation of Kaonic hydrogen K_{α} X rays. Phys. Rev. Lett. **78**, 3067–3069 (1997). <https://doi.org/10.1103/PhysRevLett.78.3067>
17. M. Bazzi et al., A new measurement of kaonic hydrogen X-rays. Phys. Lett. B **704**(3), 113 (2011). <https://doi.org/10.1016/j.physletb.2011.09.011>
18. J. Davies et al., Observation of kaonic hydrogen atom X-rays. Phys. Lett. B **83**, 55–58 (1979). [https://doi.org/10.1016/0370-2693\(79\)90887-6](https://doi.org/10.1016/0370-2693(79)90887-6)
19. M. Izycki et al., Results of the search for K-series X-rays from kaonic hydrogen. Z Physik A **297**, 11–15 (1980). <https://doi.org/10.1007/BF01414238>
20. P. Bird et al., Kaonic hydrogen atom X-rays. Nucl. Phys. A **404**, 482–494 (1983). [https://doi.org/10.1016/0375-9474\(83\)90272-5](https://doi.org/10.1016/0375-9474(83)90272-5)
21. A. Martin, Kaon-nucleon parameters. Nucl. Phys. B **179**, 33–48 (1981). [https://doi.org/10.1016/0550-3213\(81\)90247-9](https://doi.org/10.1016/0550-3213(81)90247-9)
22. J. Kim, Low-Energy $K^{-} - p$ Interaction and Interpretation of the 1405-MeV Y_0^{*} Resonance as a $\bar{K}N$ Bound State. Phys. Rev. Lett. **14**, 29–30 (1965). <https://doi.org/10.1103/PhysRevLett.14.29>
23. M. Sakitt et al., Low-energy K^{-} -meson interactions in hydrogen. Phys. Rev. **139**, B719–B728 (1965). <https://doi.org/10.1103/PhysRev.139.B719>
24. S. Baird et al., Measurements on exotic atoms of helium. Nucl. Phys. A **392**, 297–310 (1983). [https://doi.org/10.1016/0375-9474\(83\)90127-6](https://doi.org/10.1016/0375-9474(83)90127-6)
25. S. Hirenzaki et al., Chiral unitary model for the kaonic atom. Phys. Rev. C **61**, 055205 (2000). <https://doi.org/10.1103/PhysRevC.61.055205>
26. M. Bazzi et al., Measurements of the strong-interaction widths of the kaonic 3He and 4He 2p levels. Phys. Lett. B **714**, 40–43 (2012). <https://doi.org/10.1016/j.physletb.2012.06.071>
27. D. Sirghi et al., A new kaonic helium measurement in gas by SID-DHARTINO at the DAΦNE collider. J. Phys. G: Nucl. Part. Phys. **49**, 055106 (2022). <https://doi.org/10.1088/1361-6471/ac5dac>
28. C. Milardi, et al., Preparation Activity for the Siddharta-2 Run at DAΦNE, in: 9th International Particle Accelerator Conference, IPAC2018, Vancouver BC Canada, 2018. <https://doi.org/10.18429/JACoW-IPAC2018-MOPMF088>
29. M. Skurzok et al., Characterization of the SIDDHARTA-2 luminosity monitor. JINST **15**(10), P10010 (2020). <https://doi.org/10.1088/1748-0221/15/10/P10010>
30. P. Moskal et al., Simulating NEMA characteristics of the modular total-body J-PET scanner—an economic total-body PET from plastic scintillators. Phys. Med. Biol. **66**, 175015 (2021). <https://doi.org/10.1088/1361-6560/ac16bd>
31. P. Moskal, A. Gajos, M. Mohammed, and others, Testing CPT symmetry in ortho-positronium decays with positronium annihilation tomography. Nat. Commun. **12**, 5658 (2021). <https://doi.org/10.1038/s41467-021-25905-9>
32. P. Moskal et al., Positronium imaging with the novel multiphoton PET scanner. Sci. Adv. **7**, eabh4394 (2021). <https://doi.org/10.1126/sciadv.abh4394>
33. S. Niedźwiecki et al., J-PET: a new technology for the whole-body PET imaging. Acta Phys. Pol. B **48**, 1567 (2017). <https://doi.org/10.1126/sciadv.abh4394>
34. L. Bombelli, C. Fiorini, T. Frizzi, R. Nava, A. Greppi, A. Longoni, Low-noise cmos charge preamplifier for x-ray spectroscopy detectors, in: IEEE Nuclear Science Symposium Medical Imaging Conference, 2010, pp. 135–138. <https://doi.org/10.1109/NSSMIC.2010.5873732>
35. R. Quaglia, F. Schembari, G. Bellotti, A.D. Butt, C. Fiorini, L. Bombelli, G. Giacomini, F. Fiorella, C. Piemonte, N. Zorzi, Development of arrays of Silicon Drift Detectors and readout ASIC for the SIDDHARTA experiment. Nucl. Instrum. Meth. A **824**, 449–451 (2016). <https://doi.org/10.1016/j.nima.2015.08.079>
36. F. Schembari et al., SFERA: an integrated circuit for the readout of X and γ -Ray detectors. IEEE Trans. Nucl. Sci. **63**, 1797 (2016). <https://doi.org/10.1109/TNS.2016.2565200>
37. F. Sgaramella et al., The SIDDHARTA-2 calibration method for high precision kaonic atoms x-ray spectroscopy measurements. Phys. Scripta **97**(11), 114002 (2022). <https://doi.org/10.1088/1402-4896/ac95da>
38. M. Miliucci et al., Silicon drift detectors system for high-precision light kaonic atoms spectroscopy. Meas. Sci. Tech. **32**(9), 095501 (2021). <https://doi.org/10.1088/1361-6501/abeca9>
39. C. Curceanu, C. Guaraldo, M. Iliescu, M. Cargnelli, R. Hayano, J. Marton, J. Zmeskal, T. Ishiwatari, M. Iwasaki, S. Okada, D.L. Sirghi, H. Tatsuno, The modern era of light kaonic atom experiments. Rev. Mod. Phys. **91**, 025006 (2019). <https://doi.org/10.1103/RevModPhys.91.025006>
40. M. Bazzi, and others (SIDDHARTA collaboration), Kaonic helium-4 X-ray measurement in SIDDHARTA. Phys. Lett. B **681**, 310–314 (2009). <https://doi.org/10.1016/j.physletb.2009.10.052>
41. M. Miliucci et al., Large area silicon drift detectors system for high precision timed X-ray spectroscopy. Meas. Sci. Tech. **33**(9), 095502 (2022). <https://doi.org/10.1088/1361-6501/ac777a>
42. S. Wycech, B. Loiseau, An Advantage of “Upper Levels.” Acta Phys. Polon. B **51**, 109 (2020). <https://doi.org/10.5506/APhysPolB.51.109>
43. M. Merafina, F.G. Saturni, C. Curceanu, R. Del Grande, K. Piscicchia, Self-gravitating strange dark matter halos around galax-

- ies. Phys. Rev. D **102**(8), 083015 (2020). <https://doi.org/10.1103/PhysRevD.102.083015>. [arXiv:2007.03024](https://arxiv.org/abs/2007.03024)
44. C. Curceanu et al., Kaonic atoms to investigate global symmetry breaking. *Symmetry* **12**(4), 547 (2020). <https://doi.org/10.3390/sym12040547>
45. A. Drago, M. Moretti, G. Pagliara, The equation of state of dense matter: stiff, soft, or both? *Astron. Nachr.* **340**(1–3), 189–193 (2019). <https://doi.org/10.1002/asna.201913586>
46. C. Curceanu et al., Kaonic atoms measurements at DAΦNE: SIDDHARTA-2 and future perspectives. *Few Body Syst.* **62**(4), 83 (2021). <https://doi.org/10.1007/s00601-021-01666-5>
47. C. Curceanu, et al., Fundamental physics at the strangeness frontier at DAΦNE. Outline of a proposal for future measurements 4 (2021). [arXiv:2104.06076](https://arxiv.org/abs/2104.06076)

Springer Nature or its licensor (e.g. a society or other partner) holds exclusive rights to this article under a publishing agreement with the author(s) or other rightsholder(s); author self-archiving of the accepted manuscript version of this article is solely governed by the terms of such publishing agreement and applicable law.